Ca^{2+}-Induced Ca^{2+} Release through Localized Ca^{2+} Uncaging in Smooth Muscle

Guangju Ji,[1] Morris Feldman,[1] Robert Doran,[1] Warren Zipfel,[2] and Michael I. Kotlikoff[1]

[1]Department of Biomedical Sciences, College of Veterinary Medicine, and [2]Department of Engineering and Applied Physics, College of Engineering, Cornell University, Ithaca, NY 14850

Ca^{2+}-induced Ca^{2+} release (CICR) from the sarcoplasmic reticulum (SR) occurs in smooth muscle as spontaneous SR Ca^{2+} release or Ca^{2+} sparks and, in some spiking tissues, as Ca^{2+} release that is triggered by the activation of sarcolemmal Ca^{2+} channels. Both processes display spatial localization in that release occurs at a higher frequency at specific subcellular regions. We have used two-photon flash photolysis (TPFP) of caged Ca^{2+} (DMNP-EDTA) in Fluo-4–loaded urinary bladder smooth muscle cells to determine the extent to which spatially localized increases in Ca^{2+} activate SR release and to further understand the molecular and biophysical processes underlying CICR. TPFP resulted in localized Ca^{2+} release in the form of Ca^{2+} sparks and Ca^{2+} waves that were distinguishable from increases in Ca^{2+} associated with Ca^{2+} uncaging, unequivocally demonstrating that Ca^{2+} release occurs subsequent to a localized rise in $[Ca^{2+}]_i$. TPFP-triggered Ca^{2+} release was not constrained to a few discharge regions but could be activated at all areas of the cell, with release usually occurring at or within several microns of the site of photolysis. As expected, the process of CICR was dominated by ryanodine receptor (RYR) activity, as ryanodine abolished individual Ca^{2+} sparks and evoked release with different threshold and kinetics in FKBP12.6-null cells. However, TPFP CICR was not completely inhibited by ryanodine; Ca^{2+} release with distinct kinetic features occurred with a higher TPFP threshold in the presence of ryanodine. This high threshold release was blocked by xestospongin C, and the pharmacological sensitivity and kinetics were consistent with CICR release at high local $[Ca^{2+}]_i$ through inositol trisphosphate ($InsP_3$) receptors ($InsP_3Rs$). We conclude that CICR activated by localized Ca^{2+} release bears essential similarities to those observed by the activation of I_{Ca} (i.e., major dependence on the type 2 RYR), that the release is not spatially constrained to a few specific subcellular regions, and that Ca^{2+} release through $InsP_3R$ can occur at high local $[Ca^{2+}]_i$.

The Journal of General Physiology

INTRODUCTION

Sarcoplasmic release of Ca^{2+} through RYRs occurs in two prominent forms in smooth muscle: spontaneous SR Ca^{2+} release events, or Ca^{2+} sparks (Nelson et al., 1995), and Ca^{2+} release that is triggered by the influx of Ca^{2+} through sarcolemmal ion channels, often termed CICR (Imaizumi et al., 1998; Collier et al., 2000). The latter process has been shown to occur in some smooth muscle cells through processes that are generally similar to those of cardiac muscle but that bear distinct attributes (Imaizumi et al., 1998; Collier et al., 2000; Kotlikoff, 2003). Thus, in urinary bladder myocytes, activation of the voltage-dependent Ca^{2+} current (I_{Ca}) evokes CICR in the form of Ca^{2+} sparks or global Ca^{2+} waves in a graded fashion (Imaizumi et al., 1998; Collier et al., 2000). Genetic evidence indicates that type 2 RYR (RYR2) channel proteins play a predominate role in SR Ca^{2+} release in bladder myocytes (Ji et al., 2004b), which is similar to CICR in heart cells. However, CICR initiates from discrete sites in smooth muscle, and release occurs with a variable delay that depends on the flux of Ca^{2+} into the cytosol (Collier et al., 2000; Kotlikoff, 2003), which are features that are distinct from the highly amplified and spatially ordered process in cardiac cells (Cannell et al., 1995; Collier et al., 1999). Moreover, CICR in smooth muscle is a graded, nonobligate process that requires sufficient Ca^{2+} flux to activate release, leading to its description as "loose coupling" (Collier et al., 2000; Kotlikoff, 2003). Loose coupling between the activities of the sarcolemmal and SR Ca^{2+} channels suggests that unlike in cardiac muscle, where a cluster of RYR2 channels sense Ca^{2+} in the microdomain of L-type Ca^{2+} channels, RYR gating is coupled to Ca^{2+} channel activity through increases in cytosolic Ca^{2+} that must extend over a mean path length on the order of 100 nm (Collier et al., 2000). However, no studies have established the relationship between a rise in intracellular Ca^{2+} that is independent of L-type Ca^{2+} channel activity and SR release.

Two-photon flash photolysis (TPFP) provides the capability to photorelease molecules in a subcellular volume on the order of 1 femtoliter (Soeller et al., 2003), and this method has been used to examine CICR in

Correspondence to Michael I. Kotlikoff: mik7@cornell.edu

Abbreviations used in this paper: AM, acetoxymethyl ester; $InsP_3$, inositol trisphosphate; $InsP_3R$, $InsP_3$ receptor; TPFP, two-photon flash photolysis.

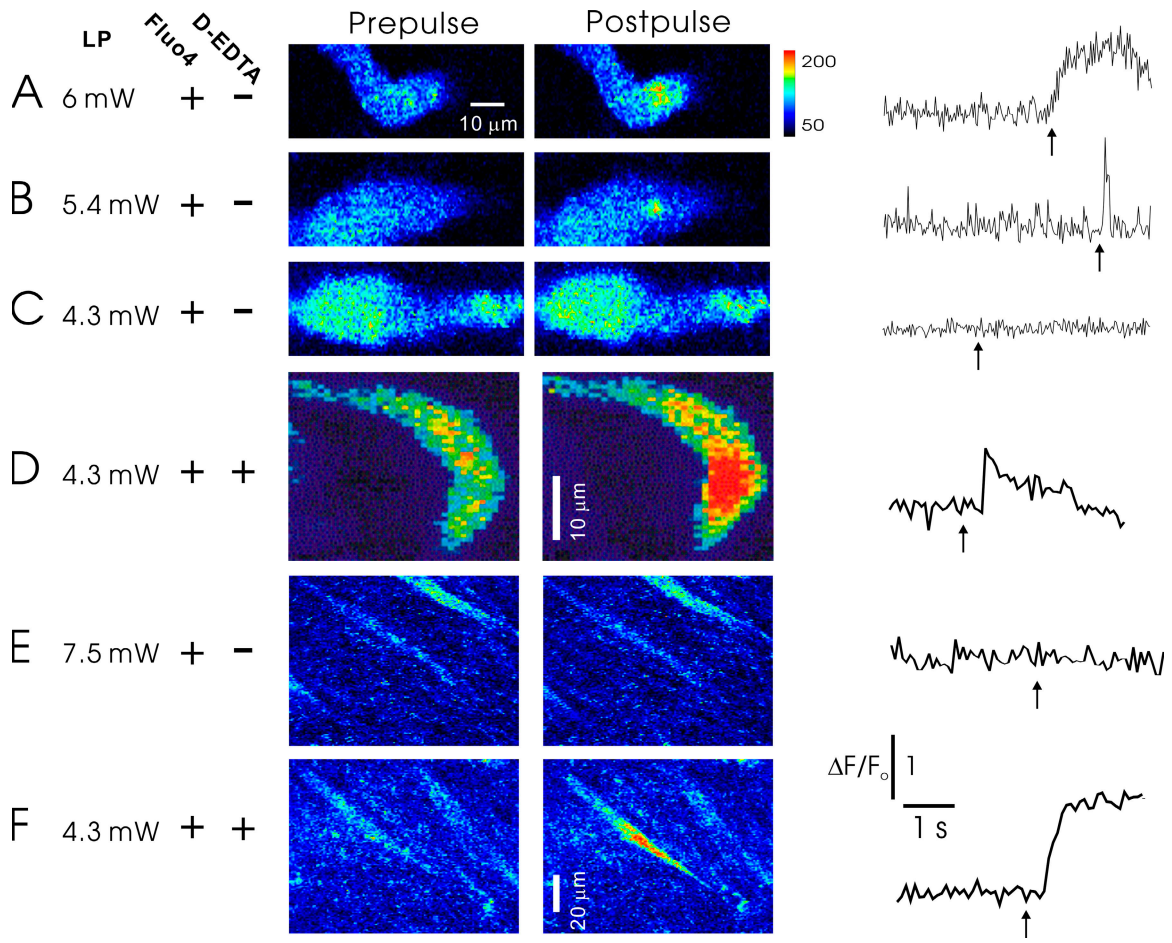

Figure 1. TPFP of caged Ca^{2+} in smooth muscle cells. Multiphoton uncaging of Ca^{2+} in smooth muscle. Cells (A–D) or tissues (E and F) were loaded with Fluo4 for the measurement of $[Ca^{2+}]_i$ and exposed to 730-nm excitation at the laser power (LP) shown under control conditions or after loading with caged Ca^{2+} (D-EDTA). At excitation power >5 mW, photodamage-induced Ca^{2+} release was observed in single cells in the absence of TPFP (no caged Ca^{2+}) but was not observed <5 mW (C). Ca^{2+} release was only observed in cells and tissues loaded with D-EDTA (compare D with C and F with E) and was evoked in single cells at laser strengths below the threshold for photodamage (compare D with C). Profiles at right show fluorescence values from entire image series at the site of photolysis. Arrows indicate point of laser flash. Excitation powers shown were measured at the objective.

heart cells (DelPrincipe et al., 1999; Lindegger and Niggli, 2005). In this study, we used TPFP to formally test several hypotheses relating to CICR in smooth muscle cells. First, we examined whether localized increases in Ca^{2+} in a small subcellular domain is sufficient to evoke Ca^{2+} release from the SR independently of the gating of sarcolemmal Ca^{2+} channels. Second, as spontaneous Ca^{2+} release often occurs at a few frequent discharge sites within myocytes (Gordienko et al., 1998), we determined the extent to which CICR is constrained to these sites. Finally, we sought to determine the extent to which TPFP could evoke Ca^{2+} release from the inositol trisphosphate ($InsP_3$) receptor ($InsP_3R$). We report that TPFP triggers CICR, that the process is not constrained to a few release sites (although Ca^{2+} sparks are often evoked several microns away from the release site), and that the process involves release through RYR2 channels. Surprisingly, however, we report evidence that TPFP also results in the release of Ca^{2+} through $InsP_3Rs$ in the absence of PLC activation and that this process, although kinetically distinct from RYR release, is capable of supporting robust CICR.

MATERIALS AND METHODS

Cell Preparations

Single-cell TPFP was performed in isolated rabbit urinary bladder myocytes, as these provided single cells with robust morphology. Single-cell isolation was performed as previously described (Collier et al., 2000). In brief, animals were sedated with xylasine and ketamine before killing with pentabarbital (protocol approved by the Cornell Institutional Animal Care and Use Committee [IACUC]). Bladders were quickly removed, cut into small pieces, and digested in enzymatic solutions. Segments were first incubated for 20 min at 37°C in buffer solution (80 mM Na-glutamate, 55 mM NaCl, 6 mM KCl, 2 mM $MgCl_2$, 10 mM HEPES, and 10 mM glucose, pH 7.4) and 1 mg/ml dithioerythreitol, 1 mg/ml papain,

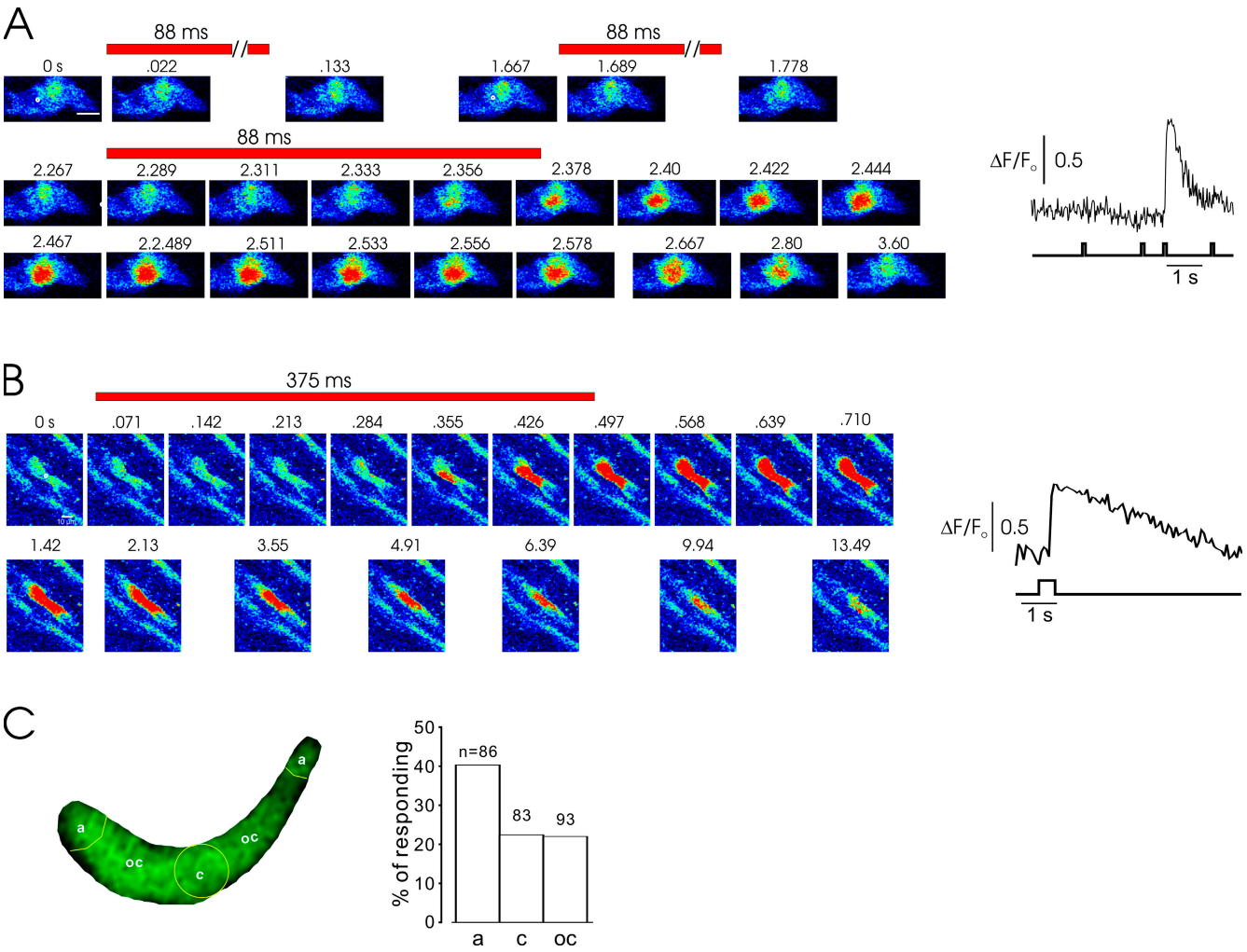

Figure 2. Ca^{2+} waves triggered by localized Ca^{2+} uncaging. (A) Typical response to 88-ms two-photon excitation (4.7 mW) shows that two initial stimuli do not result in an observed release of Ca^{2+} (i.e., photoreleased Ca^{2+} is below the threshold of detection). A third pulse at the same location results in a localized release that propagates partially throughout the cell. Three pulses were within 15 s. (B) More slowly propagating asynchronous waves were occasionally observed with longer laser pulses or multiple short pulses. In the experiment shown, a single, longer pulse activated a slowly propagating Ca^{2+} wave at the site of laser focus after ~200 ms. Note the slow time course of propagation and decay of the Ca^{2+} transient. (A and B) Bars, 10 μm. (C) Schematic showing areas in which TPFP activated Ca^{2+} release in single cells after a single 88-ms pulse. CICR was almost twofold more likely at the cell periphery. c, center; oc, off center; a, cell end.

and 1 mg/ml BSA (Sigma-Aldrich). The partially digested tissue was then transferred to the buffer solution containing 1 mg/ml collagenase type II (Worthington Biochemical), 1 mg/ml BSA, and 100 μM Ca^{2+}. After incubation for 10 min, the digested tissue was washed and gently triturated in buffer to yield single smooth muscle cells.

All intact muscle experiments were performed in mouse bladder tissue. Mice were killed with CO_2 according to a Cornell IACUC–approved protocol, and bladders were rapidly removed and dissected in cold water. Tissue segments were prepared by cutting the detrusor into 0.1 × 0.5–cm strips running along the axis from the neck to the fundus, as described previously (Ji et al., 2004a). The strips were transferred into an optical recording chamber, fixed with a Kevlar fiber retaining clip (Warner Instruments), and recorded at room temperature. The extracellular solution used for single cell and tissue strip perfusion was 137 mM NaCl, 5.4 mM KCl, 1.8 mM $CaCl_2$, 1.0 mM $MgCl_2$, 10 mM glucose, and 10 mM HEPES, pH 7.4, adjusted with NaOH.

Imaging and Local Uncaging of Caged Ca^{2+}

Single cells and intact tissue strips were coloaded with the Ca^{2+} indicator and caged Ca^{2+} by incubation with 10 μM Fluo-4 acetoxymethyl ester (AM; Invitrogen) and DMNP-EDTA–AM (Invitrogen) in a bath solution containing 0.02% pluronic acid for 10 (single cells) or 60 min (tissue) at room temperature. Fluo-4 AM fluorescence was detected by laser scanning confocal microscopy using a confocal scanhead (Radiance 2000; Bio-Rad Laboratories) coupled to a microscope (TE300; Nikon) and a 60×/1.2 NA water immersion objective (Nikon) as previously described (Ji et al., 2004b). Confocal xy images of 128 × 20 pixels were obtained at intervals of 16.7 ms. Line scan images were acquired at 1,200 Hz and 0.73 μm/pixel.

Local uncaging of DMNP-EGTA was achieved by brief exposure to the output of a diode-pumped Ti-sapphire laser (Mai Tai; Spectra-Physics) tuned to 730 nm (~100 fs pulse width). Output from the laser was directed through a computer-controlled shutter and neural density filter wheel and entered the inverted microscope

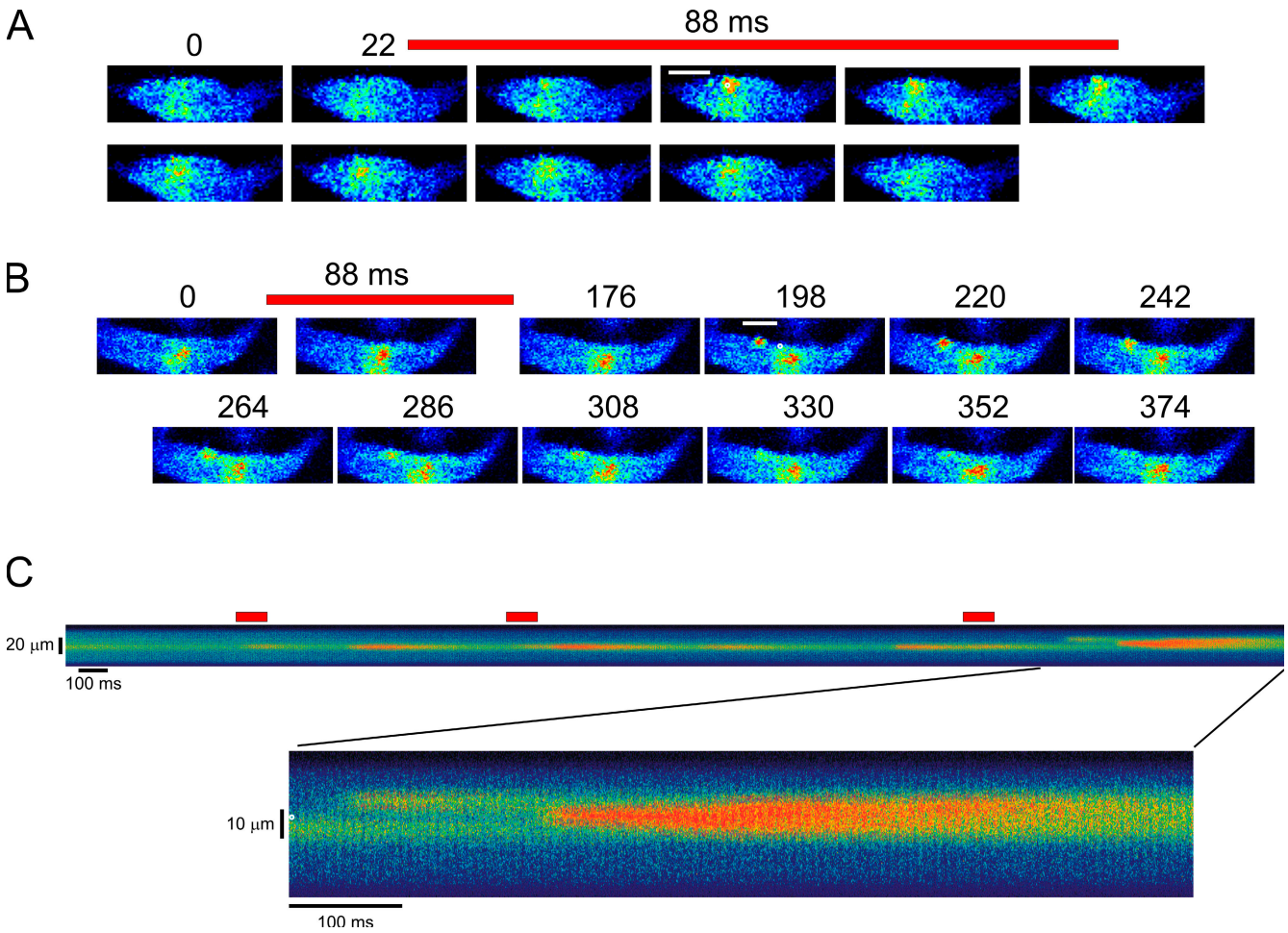

Figure 3. Activation of Ca^{2+} sparks by TPFP. (A) Sequential images obtained at 22-ms intervals before, during, and after TPFP (indicated by red bar). To show the relationship between the laser pulse focus location and the Ca^{2+} spark, the stimulation point is shown by the white circle on the image containing the scale bar. Note that the spark occurs at the site of focus of the uncaging pulse within 20 ms of the onset of the flash. (B) A similar experiment as in A, but demonstrating the activation of a Ca^{2+} spark ~6 μm from the laser focus with a delay of ~180 ms. Images taken from a series obtained at 22-ms intervals. Sequential images are shown starting with the third image, which also shows the point of laser focus (white circle). (A and B) Bars, 10 μm. (C) Line scan experiment demonstrating repeated activation of Ca^{2+} sparks with typical kinetics and spread at the site of laser focus. Ca^{2+} sparks were repeatedly triggered at the same site by a single photolysis stimulus (note first and second pulses). Inset shows last induced sparks at higher magnification and the relationship to the site of laser photolysis (white circle). Note the activation of separate Ca^{2+} sparks at ~5 μm from the point of laser focus.

(TE300; Nikon) through a modification of the epifluorescence illumination port. The coupling optics included a moveable lens to adjust the focus of the 730-nm light so that its focus was coincident with the focal plane of the 488-nm imaging excitation. This was verified by comparison of the axial position of the photobleached focal region after a brief bleaching pulse from each laser. Images were processed and analyzed using MATLAB 6.5 software (MathWorks). Data are reported as means ± SEM. A *t* test was applied to determine the statistical significance of measured differences.

Analysis

Kinetic data were calculated by fits of the data using custom software written in MATLAB that fit fluorescence data to a six-parameter equation (F_0, start time, rise time, peak F/F_0, half-time of decay, and final offset using a nonlinear least squares fitting routine; Ji et al., 2004b). Rise times indicate the period of time from 10 to 90% of the event fitted from baseline to peak F/F_0. Ca^{2+} propagation velocity was determined by individually calculating the time required to traverse a distance of at least 20 μm in the calibrated images. Mean results are expressed as means ± SEM. Statistical analysis was performed by ANOVA.

RESULTS

Local Uncaging of Caged Ca^{2+} Induces Ca^{2+} Release in Smooth Muscle

We first examined the toxicity of two-photon excitation in single smooth muscle cells or tissue segments by exciting Fluo-4–loaded myocytes at varying power. As shown in Fig. 1, in the absence of DMNP-EDTA, excitation pulses for 100 ms produced localized increases in Ca^{2+} in isolated smooth muscle cells and tissues only at

powers above 5 mW, indicating localized membrane damage. At 4.3 mW, however, no increase in Fluo-4 fluorescence was observed in the absence of DMNP-EDTA in either single-cell (Fig. 1 C) or tissue (Fig. 1 E) experiments, and excitation energies were accordingly confined to powers of <4.3 for 100 ms or shorter. Conversely, in Fluo-4/DMNP-EDTA–loaded cells or tissues, a 100-ms pulse at 4.3 mW produced robust Ca^{2+} responses in individual myocytes, indicating that these parameters were sufficient to produce effective two-photon uncaging. The pattern of rise in Ca^{2+} after short laser pulses was either a rapid Ca^{2+} flash, consisting of a nearly synchronous rise in Ca^{2+} throughout the cell (Fig. 1 E), or an asynchronous Ca^{2+} wave, which propagated more slowly throughout the cell (Fig. 1 F).

We next sought to determine whether the rise in Fluo-4 fluorescence in DMNP-EDTA–loaded cells resulted from the uncaging of Ca^{2+} within a confined space and diffusion throughout the cell or was produced by the uncaging of a small amount of "trigger" Ca^{2+} leading to CICR. As shown in Fig. 2, cells within muscle segments were repeatedly exposed to TPFP to examine the extent to which uncaging pulses would itself produce an increase in Fluo-4 fluorescence. At uncaging stimuli below the threshold for cell damage, single pulses either produced no localized Fluo-4 fluorescence or a large Ca^{2+} release event as shown in Fig. 1, indicating that uncaging stimuli themselves did not result in a rise in Ca^{2+} sufficient enough to be detected. In situations in which a single stimulus did not result in Ca^{2+} release, repeated uncaging at the same location almost always elicited release (Fig. 2 A); CICR triggered by multiple TPFP pulses could suggest a threshold for Ca^{2+} release or might indicate that initial TPFP pulses augmented SR loading. SR loading was not required for TPFP-induced CICR, however, as single pulses were often sufficient to elicit Ca^{2+} release. These results indicated that the release of Ca^{2+} by TPFP is sufficient to evoke Ca^{2+} release from intracellular stores and that observed global increases in $[Ca^{2+}]_i$ do not result either from damage to the cell wall or simply from the uncaging of DMNP-EDTA.

As uncaging of threshold amounts of Ca^{2+} triggered release in some, but not all cases, we examined the distribution of sites from which release occurred. Using a motorized stage, single cells were systematically positioned with the beam focused on the cell regions shown in Fig. 2 C and exposed to 100 ms TPFP. Single uncaging pulses were roughly twice as likely to result in global Ca^{2+} release in the cell periphery as in the center or perinuclear regions of the cell. This may relate to the smaller volume at the cell ends and a resultant higher free $[Ca^{2+}]_i$ as a result of restricted diffusion. Global Ca^{2+} release could be evoked, however, from any region of the cell, including the cell ends, and the propagated release events extended from these regions throughout the myocytes.

To further examine the relationship between the site of TPFP and Ca^{2+} release, single cells were stimulated by TPFP and scanned in rapid xy or line scan mode. As shown in Fig. 3, Ca^{2+} photolysis often evoked typical Ca^{2+} sparks that were not propagated as larger Ca^{2+} waves; these events occurred with variable delay either during or after the uncaging stimulus, and multiple release events were often observed in line scan experiments (Fig. 3 B). The mean rise time and decay half-time were 31.1 ± 14.8 and 113.9 ± 43.6 ms, respectively; spark size was 5.41 ± 0.75 μm (full width and half maximal), and the mean amplitude ($\Delta F/F_o$) was 1.8 ± 0.1 units ($n = 9$). These values are quite similar to spontaneous Ca^{2+} sparks in rabbit urinary bladder myocytes (Collier et al., 2000; Ji et al., 2002). Ca^{2+} sparks were never observed in the presence of ryanodine, further indicating that TPFP acts at least partially by gating RYR (see Fig. 4). Although TPFP-triggered Ca^{2+} sparks were often observed at the point of focus of the TPFP beam in both xy and line scan experiments (Fig. 3, A and C), sparks were also sometimes evoked at a distance of up to 10 μm from the beam focal point (Fig. 3, B and C). Similar results were obtained in line scan experiments (Fig. 3 C), which revealed that TPFP often evoked release from sites separated by several microns. The observed latencies between the onset of the TPFP stimulus and the appearance of a Ca^{2+} spark likely reflects variability in the loading and deesterification of DMNP-EDTA as well as the diffusion time to the Ca^{2+} release site. In line scan experiments in which release occurred within 3 μm of the beam focus, the mean delay between the start of photolysis and the appearance of a Ca^{2+} spark was 16.33 ± 8.02 ms ($n = 6$). The induction of Ca^{2+} sparks that are spatially and temporally separated from the point of TPFP suggests a degree of localization of release sites or differential Ca^{2+} sensitivity of these sites. Furthermore, the localization of these sites relative to the point of TPFP (usually within 5 μm), although not consistent with only a few cellular frequent discharge sites, generally agrees with the observed number of small spontaneous Ca^{2+} spark sites in smooth muscle cells (Gordienko et al., 1998; Kirber et al., 2001).

Inhibition of Intracellular Ca^{2+} Release Channels

Previous studies have indicated that RYR gating underlies Ca^{2+} sparks in smooth muscle (Nelson et al., 1995; Mironneau et al., 1996; Gordienko et al., 1998; ZhuGe et al., 1998; Herrera and Nelson, 2002) and CICR triggered by activation of the voltage-dependent Ca^{2+} current (Imaizumi et al., 1998; Collier et al., 2000; Ji et al., 2004b), as both processes are eliminated by preexposure of cells to ryanodine. We used a similar approach to determine whether Ca^{2+} release by TPFP was ablated by the inhibition of RYR function in smooth muscle segments from the mouse detrusor. Surprisingly, the

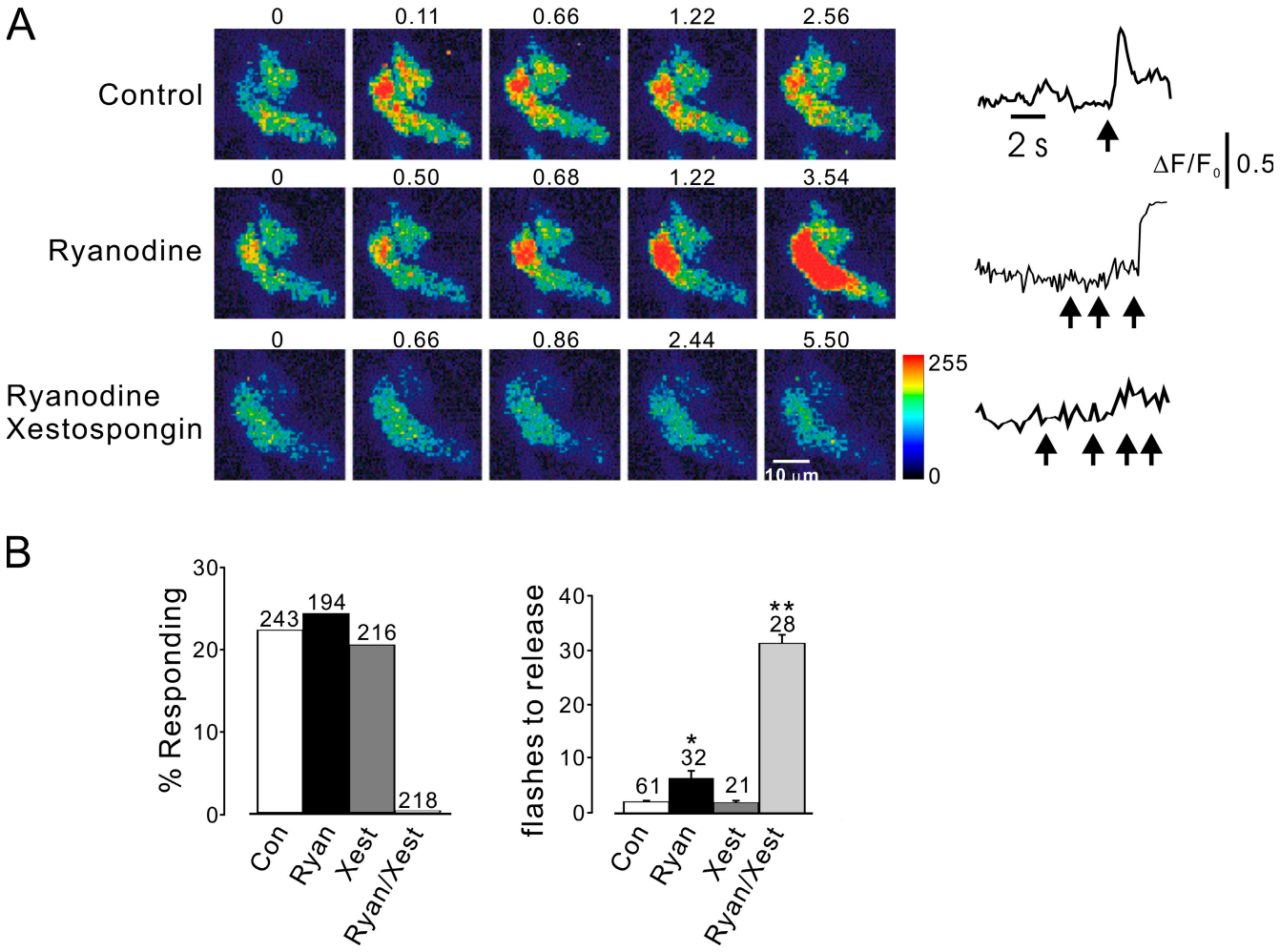

Figure 4. Ryanodine and $InsP_3Rs$ can mediate TPFP-induced CICR. (A) Incubation of cells in 10 μM ryanodine did not prevent cells from releasing Ca^{2+}, whereas combined exposure to 30 μM ryanodine and xestospongin C completely eliminated Ca^{2+} release. Arrows indicate laser flashes. (B) Summary data indicating the propability of release in each condition. Note that the number of exposures to TPFP required to induce release was significantly higher in the presence of ryanodine. Error bars represent SD. *, $P < 0.05$; **, $P < 0.01$.

application of ryanodine (10–30 μm) did not completely block Ca^{2+} release but rather markedly altered the characteristics of CICR. TPFP triggered prominent asynchronous Ca^{2+} waves in myocytes after prolonged exposure to ryanodine (Fig. 4 A). The slow rate of Ca^{2+} wave propagation in these experiments differed markedly from that observed in the absence of ryanodine and strongly suggested the involvement of $InsP_3Rs$ in CICR. The number of TPFP pulses at fixed power required to elicit CICR in the presence of ryanodine was significantly greater than in control experiments, suggesting a higher local Ca^{2+} threshold for release during RYR inhibition ($P < 0.05$; Fig. 4 B). In contrast, the exposure of segments to 30 μM xestogspongin C, an inhibitor of $InsP_3Rs$, had little effect on the probability of observing CICR or the characteristics of release in the absence of drug. That is, localized Ca^{2+} release events similar to control conditions were observed in the presence of xestospongin C. However, combined inhibition of both Ca^{2+} release channels by ryanodine and xestospongin C effectively prevented all Ca^{2+} release, indicating an effective inhibition of $InsP_3Rs$ by the antagonist and further suggesting that either intracellular Ca^{2+} release channel can support Ca^{2+} release, albeit with markedly different properties.

To further understand the role of specific intracellular Ca^{2+} release channels in locally elicited CICR, we analyzed the kinetics (rise time and time to release), Ca^{2+} wave propagation velocity, and peak amplitude of Ca^{2+} release after TPFP. The rise time of Ca^{2+} release was markedly affected by RYR antagonism, which is likely associated with a decrease in the underlying rate of SR Ca^{2+} release. Ca^{2+} spark rise time (time to 50% maximum amplitude) more than doubled in the presence of 10 μM ryanodine (155.3 ± 20.9 ms [$n = 31$] vs. 60.0 ± 5.83 ms [$n = 42$] in control experiments; Fig. 5, A and B). Conversely, in the presence of 30 μM xestospongin C, the rate of Ca^{2+} rise after TPFP (65.3 ± 5.63 ms

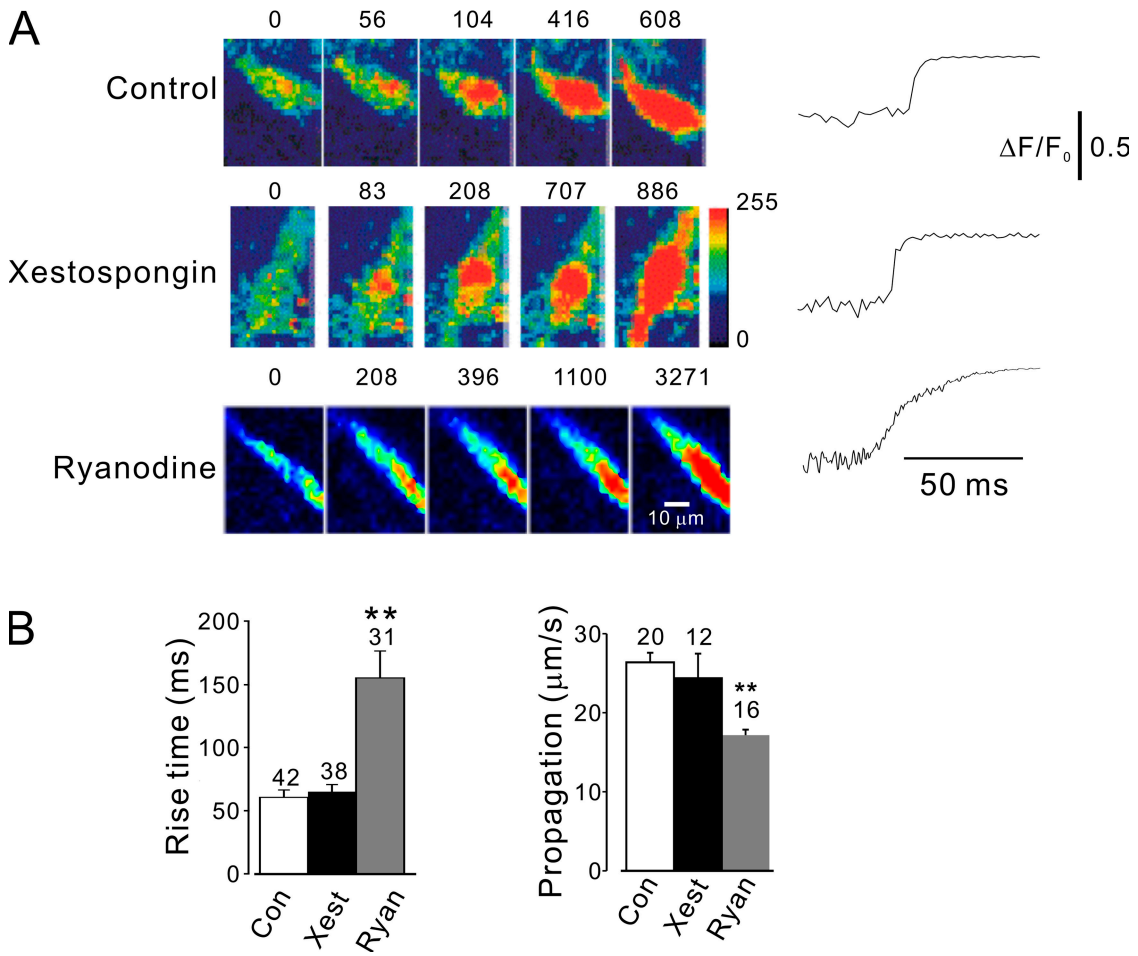

Figure 5. Altered properties of Ca^{2+} release by ryanodine and $InsP_3Rs$. (A) Examples of TPFP experiments in tissues in the three conditions. Traces at right indicate fluorescence at the laser focus site throughout continuous experiments. Note the slow rise time in the presence of ryanodine. (B) Summary data from all similar experiments. Rise time and propagation were significantly slower in the presence of ryanodine, whereas xestospongin C had no significant effect. **, $P < 0.01$. Error bars represent SD.

[$n = 38$]) was not significantly different than that of control. As shown in Figs. 4 and 5, RYR inhibition also markedly slowed the rate of Ca^{2+} wave propagation after TPFP. Wave propagation velocity decreased from 21.9 ± 1.0 μm/s ($n = 20$) to 14.3 ± 0.6 μm/s ($n = 16$) in the presence of ryanodine, whereas in the presence of xestospongin C, wave propagation was not significantly different from control (20.2 ± 2.6 $\mu m/s^{-1}$ [$n = 16$]; Fig. 5, A and C).

Similarly, localized Ca^{2+} photolysis in the presence of ryanodine delayed initiation of the Ca^{2+} release event after the TPFP pulse. To more effectively quantify the time to release, cells within intact muscle segments were exposed to light for 100 ms (4.3 mW) at the beginning of a prolonged x-t scan along the cell axis, and the time delay was calculated as the time from the beginning of the 730-nm pulse to the initiation of Ca^{2+} release. The time to release was doubled in the presence of 30 μM ryanodine (123.3 ± 5.7 ms [$n = 23$] vs. 217.3 ± 11.4 ms [$n = 31$] for control and ryanodine, respectively), whereas the inhibition of $InsP_3Rs$ with xestospongin C had no significant effect ($P > 0.05$; 129.9 ± 7.41 ms [$n = 17$]; Fig. 6). Because release occurred after completion of the TPFP pulse, the increased delay associated with RYR inhibition could not be caused by a requirement for greater net Ca^{2+} uncaging. Rather, the delay likely indicates an increased time requirement for the spread of the local rise in Ca^{2+}, although it is also possible that the opening of more individual $InsP_3$ channels is necessary to generate an observable response. Although the probability of observing CICR after TPFP and the rate of initiation and development of the Ca^{2+} release were markedly affected by RYR antagonism, the peak level of Ca^{2+} achieved was not significantly affected. The amplitude of the Ca^{2+} spark or Ca^{2+} wave was equivalent in control cells and those incubated with 10 μM ryanodine or 30 μM xestospongin C (Fig. 6 C), suggesting that efficient release of SR Ca^{2+} stores is achieved when CICR occurs through the activation of either SR release channel.

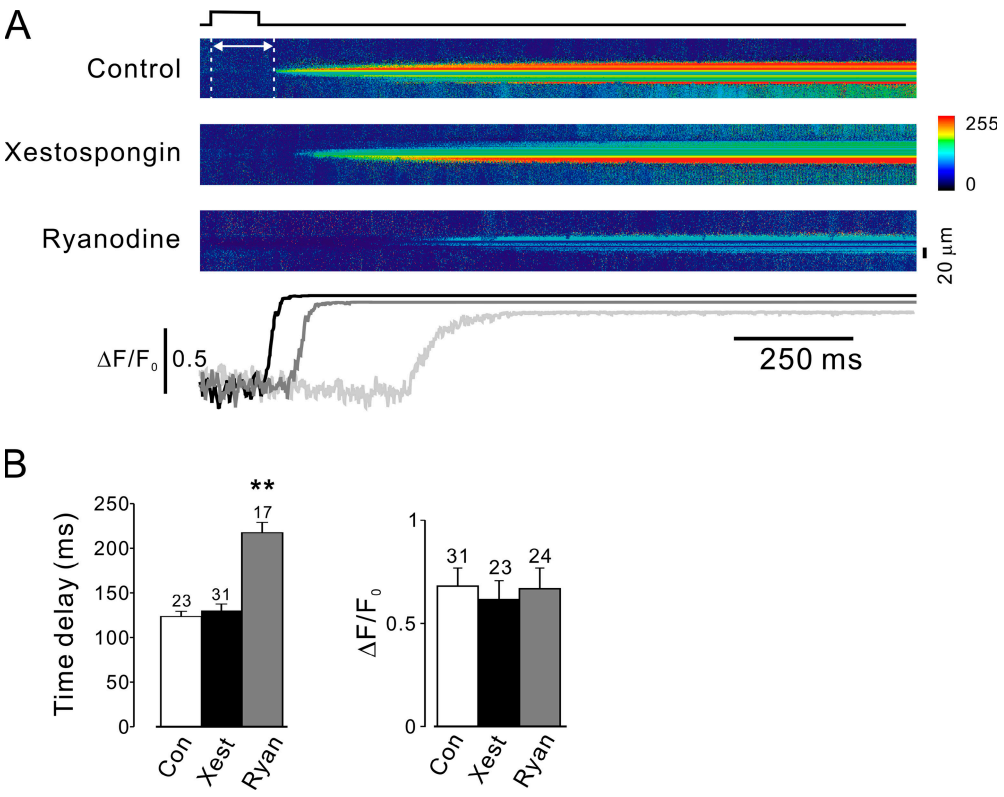

Figure 6. Increased delay to release by $InsP_3Rs$. (A) Examples of line scan experiments obtained during TPFP. Plots below indicate continuous fluorescence at the peak of release for each condition. Ryanodine markedly increased the delay between initiation of the laser uncaging flash and initial Ca^{2+} release. Laser excitation pulse was 100 ms in all experiments. As observed in xy experiments, rise time was markedly slowed in the presence of ryanodine. (B) Summary data from a series of line scan experiments indicates significant increase in delay in the presence of ryanodine. **, $P < 0.01$. Error bars represent SD.

RYR Subtype 2 (RYR2) Mediates TPFP-Induced Ca^{2+} Release in Smooth Muscle

We have previously shown that Ca^{2+} sparks activated by CICR are predictably altered in bladder myocytes from FKBP12.6- but not RYR3-deficient mice (Ji et al., 2004b). As FKBP12.6 proteins selectively associate and regulate Ca^{2+} release from RYR2 channels (Timerman et al., 1996; Xin et al., 1999), these data provide evidence that the cardiac type RYR (RYR2) plays a prominent role in the regulation of Ca^{2+} release events in smooth muscle. We used a similar strategy to determine whether TPFP activates RYR2 channels by examining TPFP-evoked Ca^{2+} release in bladder smooth muscle segments from control, FKBP12.6-null, and RYR3-null mice. As shown in Fig. 7, TPFP in FKBP12.6 knockout mice showed distinct features relative to control mice. First, the delay between the beginning of 730-nm excitation and the observation of Ca^{2+} release was markedly decreased in FKBP12.6-null tissues (Fig. 7, A and C), which is consistent with the dysregulation of RYR2 channels observed in cardiac myocytes from these mice (Xin et al., 2002). Second, Ca^{2+} spark/wave propagation speed was increased relative to wild-type myocytes, with the rate of propagation significantly higher in FKBP12.6 knockout mice (30.7 vs. 21.9 µm/s; $P < 0.01$; Fig. 7, B and C). Exposure of FBKP12.6-null myocytes to ryanodine dramatically decreased the propagation rate to 9.0 ± 0.7 µm/s ($n = 16$; not depicted), which is consistent with effects on propagation in wild-type cells. The rise time for Ca^{2+} sparks was significantly faster in FKBP12.6-null tissues (41.7 ± 1.64 vs. 60.9 ± 5.83 ms; $P < 0.01$; Fig. 7). The maximum amplitude of Ca^{2+} release was not significantly different from control experiments. The marked alteration in kinetic properties of locally induced CICR is consistent with a major role of RYR2 proteins in the initial release (delay and rise time) as well as propagation of the Ca^{2+} wave.

DISCUSSION

We report that localized photolysis of caged Ca^{2+} initiates CICR in urinary bladder myocytes, which is the first demonstration that a local increase in cytosolic $[Ca^{2+}]_i$ in the absence of depolarizing voltage steps and/or the gating of sarcolemmal ion channels is sufficient to activate single Ca^{2+} sparks and propagating Ca^{2+} waves. The finding that localized photolysis of cytosolic DMNP-EDTA triggers individual Ca^{2+} sparks that are propagated throughout the cell (Figs. 1 and 2 A) and that this process often requires multiple excitation pulses further supports the mechanistic interpretation underlying the delay that can be observed between membrane depolarization and Ca^{2+} release during triggered CICR in smooth muscle (Collier et al., 2000). That is, CICR triggered by the activation of I_{Ca} requires a sufficient increase in $[Ca^{2+}]$ to activate Ca^{2+} release channels, which is in contrast to the highly localized, tightly coupled process that occurs at the cardiac triad (Collier et al., 1999).

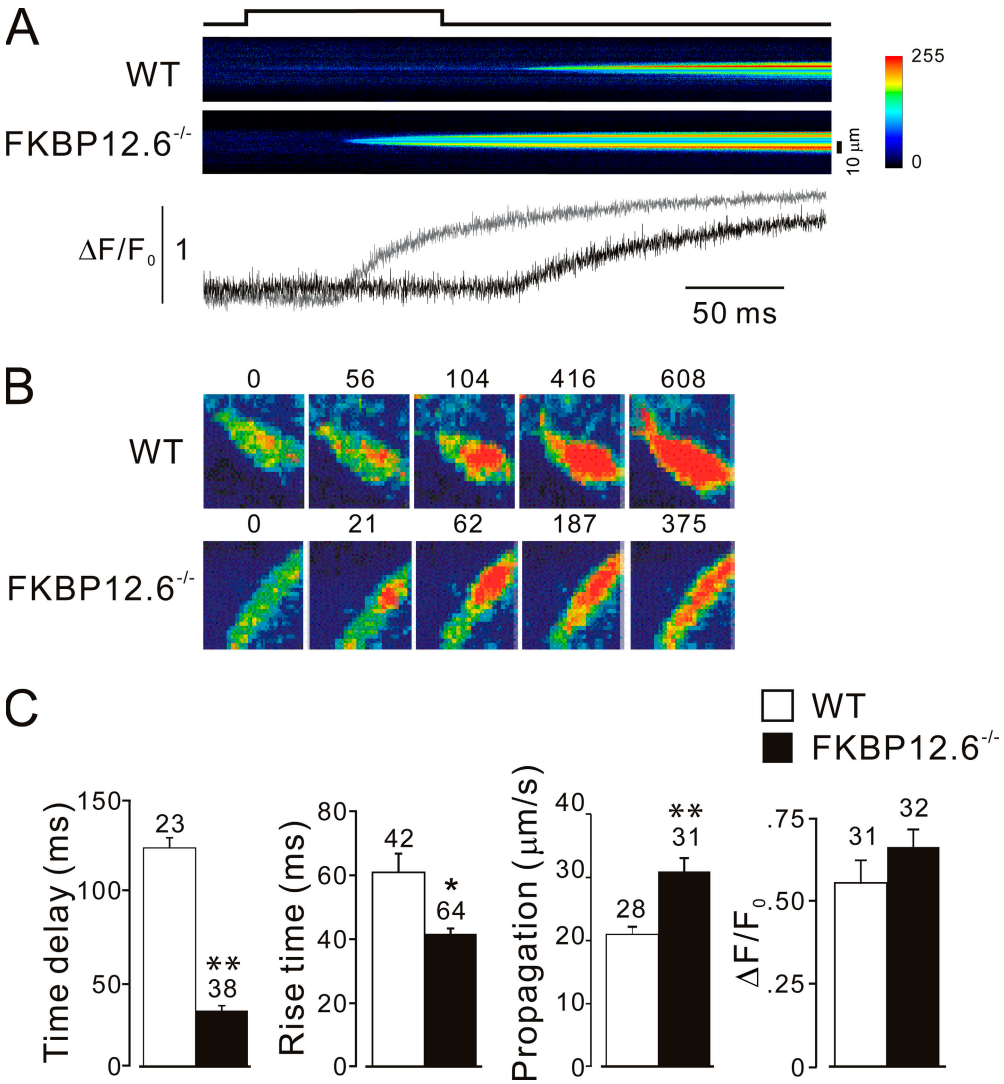

Figure 7. FKBP12.6 inactivation alters TPFP Ca^{2+} release. (A) Line scan experiments indicate a decrease in delay from initiation of the photolysis pulse to the observation of Ca^{2+} release. (B) Sequential xy images also indicate earlier release in FKBP12.6-null myocytes. Note different time scales. (C) Summary data indicate the marked change in kinetics of Ca^{2+} release in FKBP12.6-null tissues. *, $P < 0.05$; **, $P < 0.01$. Error bars represent SD.

Activation of CICR by TPFP also provides a formal demonstration that the gating of voltage-dependent Ca^{2+} channels, which display high amplitude currents and a measurable open probability at resting voltages in smooth muscle and support the activation of spontaneous Ca^{2+} sparks (Gollasch et al., 1992; Fleischmann et al., 1994), is not a necessary factor in RYR gating in smooth muscle.

Despite the tendency of large spontaneous Ca^{2+} sparks to occur at a few frequent discharge sites (Gordienko et al., 1998), we did not observe this phenomenon with TPFP. Ca^{2+} release could be evoked throughout all regions of the cell, and spark initiation sites usually occurred at or near the site of laser focus rather than at one of the several observed spontaneous release sites. These results suggest that the phenomenon of frequent discharge sites may not arise solely as a result of the clustering of a few highly specialized or concentrated SRs and that release can occur from a relatively homogenously distributed SR. In support of this conclusion, 730-nm pulses activated Ca^{2+} release with a similar delay as observed in cardiac myocytes (between 10 and 100 ms; Lipp and Niggli, 1998), suggesting that the mean path for released Ca^{2+} ions to traverse within the cytosol is not markedly longer in smooth muscle (assuming a similar rate of rise of Ca^{2+} during photolysis). However, several factors suggest caution regarding this interpretation. First, as shown in Fig. 3, it was possible to evoke Ca^{2+} sparks at a distance of up to ~5 µm from the site of beam focus, and these events occurred with a delay in excess of 100 ms and are consistent with delays reported by the submaximal activation of I_{Ca} (Collier et al., 2000). Although it is difficult to directly compare the latency to first spark in these two circumstances because the rate of rise of $[Ca^{2+}]_i$ produced by TPFP is not known, the delay and spatial separation between the point of beam focus and point of Ca^{2+} spark activation suggests a degree of spatial organization unlike that observed in cardiac myocytes. Second, the presence of a ryanodine-insensitive component of Ca^{2+} release

substantially complicates this analysis. It is possible, for example, to explain the results by a clustering of RYR release sites at ~10-μm intervals throughout smooth muscle cells but with substantially more homogenously expressed $InsP_3R$, a finding that is generally supported by immunocytochemical studies (Nakanishi, et al., 1996; Lesh et al., 1998). Finally, it should be noted that although frequent discharge sites may reflect characteristics of the SR, it is also possible that these sites reflect regions of sustained sarcolemmal Ca^{2+} channel activity (Navedo et al., 2005).

The most surprising finding in our study was the apparent ability of TPFP to activate Ca^{2+} release through $InsP_3Rs$, as indicated by the activation of Ca^{2+} that occurred with different kinetics (delay, rise time, and propagation) and required greater amounts of trigger Ca^{2+} in the presence of 10 μM ryanodine. The activation of slowly propagating asynchronous Ca^{2+} waves in the presence of ryanodine, the marked slowing of wave propagation velocity in the presence of ryanodine, and the complete inhibition of TPFP in the presence of xestospongin C and ryanodine but not in the presence of ryanodine alone strongly suggest that $InsP_3R$ Ca^{2+} release can be activated by local increases in $[Ca^{2+}]_i$. Although substantial data indicate that the gating of $InsP_3R$ is augmented by increases in cytosolic Ca^{2+} at lower levels of Ca^{2+} (Iino and Endo, 1992; Iino et al., 1993), this process has been considered insufficient to activate $InsP_3R$ gating in the absence of $InsP_3$ and relief of Ca^{2+} inhibition of gating (Taylor, 1998). However, $InsP_3R$ gating by Ca^{2+} may be a function of the level of basal PLC activity in cells or the specific patterns of $InsP_3R$ subtype expression and the formation of heterotetrameric channels (Joseph et al., 1995). The activation of $InsP_3R$ by TPFP may reflect the gating of these channels by high local increases in $[Ca^{2+}]_i$, particularly as Ca^{2+} release required multiple laser pulses in the presence of ryanodine (Fig. 4) and as xestospongin C alone had little effect on Ca^{2+} release, although this notion appears inconsistent with the well-known inhibitory effect of high Ca^{2+} on $InsP_3R$ gating (Bezprozvanny et al., 1991). Although our findings suggest that RYRs dominate the pattern of Ca^{2+} release after local rises in $[Ca^{2+}]_i$, the ability to trigger release from $InsP_3R$ suggests the potential for some involvement of these release channels during CICR, as release through RYR gating would be expected to produce very high local concentrations of Ca^{2+}.

Finally, our data further indicate the importance of RYR2 channel subtypes in CICR. TPFP-activated Ca^{2+} release displayed distinct characteristics in myocytes from FKBP12.6 knockout mice (Fig. 7). As FKBP12.6 proteins selectively associate with RYR2 channels (Timerman et al., 1996; Xin et al., 1999; Wang et al., 2003), the observed effects suggest that loss of the stabilizing action of FKBP12.6 on RYR2 channels (Marx et al., 2001; Xin et al., 2002) accounts for the decreased threshold (decrease in time to release) and more rapid kinetics (decreased rise time and increased propagation velocity) in myocytes from FKBP12.6-null mice. Moreover, these findings are consistent with an increase in the frequency of spontaneous Ca^{2+} sparks observed in FKBP12.6-deficient urinary bladder myocytes (Ji et al., 2004b). The marked decrease in the delay between the onset of local photolysis and the observation of Ca^{2+} release in FKBP12.6-null mice suggests that FKBP12.6 binding to RYR2 lowers the sensitivity of these channels to gating by increases in $[Ca^{2+}]_i$. The considerable decrease in rise time of the observed release is also consistent with this interpretation. Similarly, such an increase in sensitivity would be expected to increase the wave propagation rate, as adjacent release channels would be expected to be gated after less Ca^{2+} release from adjacent channels. The extent to which loss of interactions between FKBP12.6 and RYR2 underlie pathological changes in excitation–contraction coupling in smooth muscle remains to be determined.

We thank Jason Wilson, Shaun Reining, and Jane Lee for technical support.

This work is supported by National Institutes of Health grants DK065992 and HL045239.

Angus C. Nairn served as editor.

Submitted: 5 October 2005
Accepted: 2 February 2006

REFERENCES

Bezprozvanny, I., J. Watras, and B.E. Ehrlich. 1991. Bell-shaped calcium-response curves of $Ins(1,4,5)P_3$ and calcium-gated channels from endoplasmic reticulum of cerebellum. *Nature.* 351:751–754.

Cannell, M.B., H. Cheng, and W.J. Lederer. 1995. The control of calcium release in heart muscle. *Science.* 268:1045–1049.

Collier, M.L., A.P. Thomas, and J.R. Berlin. 1999. Relationship between L-type Ca2+ current and unitary sarcoplasmic reticulum Ca2+ release events in rat ventricular myocytes. *J. Physiol.* 516:117–128.

Collier, M.L., G. Ji, Y. Wang, and M.I. Kotlikoff. 2000. Calcium-induced calcium release in smooth muscle: loose coupling between the action potential and calcium release. *J. Gen. Physiol.* 115:653–662.

DelPrincipe, F., M. Egger, G.C. Ellis-Davies, and E. Niggli. 1999. Two-photon and UV-laser flash photolysis of the Ca2+ cage, dimethoxynitrophenyl-EGTA-4. *Cell Calcium.* 25:85–91.

Fleischmann, B.K., R.K. Murray, and M.I. Kotlikoff. 1994. Voltage window for sustained elevation of cytosolic calcium in smooth muscle cells. *Proc. Natl. Acad. Sci. USA.* 91:11914–11918.

Gollasch, M., J. Hescheler, J.M. Quayle, J.B. Patlak, and M.T. Nelson. 1992. Single calcium channel currents of arterial smooth muscle at physiological calcium concentrations. *Am. J. Physiol.* 263:C948–C952.

Gordienko, D.V., T.B. Bolton, and M.B. Cannell. 1998. Variability in spontaneous subcellular calcium release in guinea-pig ileum smooth muscle cells. *J. Physiol.* 507:707–720.

Herrera, G.M., and M.T. Nelson. 2002. Differential regulation of SK and BK channels by Ca(2+) signals from Ca(2+) channels

and ryanodine receptors in guinea-pig urinary bladder myocytes. *J. Physiol.* 541:483–492.

Iino, M., and M. Endo. 1992. Calcium-dependent immediate feedback control of inositol 1,4,5-triphosphate-induced Ca2+ release. *Nature.* 360:76–78.

Iino, M., T. Yamazawa, Y. Miyashita, M. Endo, and H. Kasai. 1993. Critical intracellular Ca2+ concentration for all-or-none Ca2+ spiking in single smooth muscle cells. *EMBO J.* 12:5287–5291.

Imaizumi, Y., Y. Torii, Y. Ohi, N. Nagano, K. Atsuki, H. Yamamura, K. Muraki, M. Watanabe, and T.B. Bolton. 1998. Ca2+ images and K+ current during depolarization in smooth muscle cells of the guinea-pig vas deferens and urinary bladder. *J. Physiol.* 510:705–719.

Ji, G., R.J. Barsotti, M.E. Feldman, and M.I. Kotlikoff. 2002. Stretch-induced calcium release in smooth muscle. *J. Gen. Physiol.* 119:533–544.

Ji, G., M.E. Feldman, K.Y. Deng, K.S. Greene, J. Wilson, J.C. Lee, R.C. Johnston, M. Rishniw, Y. Tallini, J. Zhang, et al. 2004a. Ca2+-sensing transgenic mice: postsynaptic signaling in smooth muscle. *J. Biol. Chem.* 279:21461–21468.

Ji, G., M.E. Feldman, K.S. Greene, V. Sorrentino, H.B. Xin, and M.I. Kotlikoff. 2004b. RYR2 proteins contribute to the formation of Ca(2+) sparks in smooth muscle. *J. Gen. Physiol.* 123:377–386.

Joseph, S.K., C. Lin, S. Pierson, A.P. Thomas, and A.R. Maranto. 1995. Heteroligomers of type-I and type-III inositol trisphosphate receptors in WB rat liver epithelial cells. *J. Biol. Chem.* 270:23310–23316.

Kirber, M.T., E.F. Etter, K.A. Bellve, L.M. Lifshitz, R.A. Tuft, F.S. Fay, J.V. Walsh Jr., and K.E. Fogarty. 2001. Relationship of Ca2+ sparks to STOCs studies with 2D and 3D imaging in feline oesophageal smooth muscle cells. *J. Physiol.* 531:315–327.

Kotlikoff, M.I. 2003. Calcium-induced calcium release in smooth muscle: the case for loose coupling. *Prog. Biophys. Mol. Biol.* 83:171–191.

Lesh, R.E., G.F. Nixon, S. Fleischer, J.A. Airey, A.P. Somlyo, and A.V. Somlyo. 1998. Localization of ryanodine receptors in smooth muscle. *Circ. Res.* 82:175–185.

Lindegger, N., and E. Niggli. 2005. Paradoxical SR Ca2+ release in guinea-pig cardiac myocytes after beta-adrenergic stimulation revealed by two-photon photolysis of caged Ca2+. *J. Physiol.* 565:801–813.

Lipp, P., and E. Niggli. 1998. Fundamental calcium release events revealed by two-photon excitation photolysis of caged calcium in Guinea-pig cardiac myocytes. *J. Physiol.* 508:801–809.

Marx, S.O., J. Gaburjakova, M. Gaburjakova, C. Henrikson, K. Ondrias, and A.R. Marks. 2001. Coupled gating between cardiac calcium release channels (ryanodine receptors). *Circ. Res.* 88:1151–1158.

Mironneau, J., S. Arnaudeau, N. Macrez-Lepretre, and F.X. Boittin. 1996. Ca2+ sparks and Ca2+ waves activate different Ca(2+)-dependent ion channels in single myocytes from rat portal vein. *Cell Calcium.* 20:153–160.

Nakanishi, S. A. Fujii, S. Nakade, and K. Mikoshiba. 1996. Immunohistochemical localization of inositol 1,4,5,-trisphosphate receptors in non-neural tissues, with special reference to epithelia, the reproductive system, and muscular tissues. *Cell Tissue Res.* 285:235–251.

Navedo, M.F., G.C. Amberg, V.S. Votaw, and L.F. Santana. 2005. Constitutively active L-type Ca2+ channels. *Proc. Natl. Acad. Sci. USA.* 102:11112–11117.

Nelson, M.T., H. Cheng, M. Rubart, L.F. Santana, A.D. Bonev, H.J. Knot, and W.J. Lederer. 1995. Relaxation of arterial smooth muscle by calcium sparks. *Science.* 270:633–637.

Soeller, C., M.D. Jacobs, K.T. Jones, G.C. Ellis-Davies, P.J. Donaldson, and M.B. Cannell. 2003. Application of two-photon flash photolysis to reveal intercellular communication and intracellular Ca2+ movements. *J. Biomed. Opt.* 8:418–427.

Taylor, C.W. 1998. Inositol trisphosphate receptors: Ca2+-modulated intracellular Ca2+ channels. *Biochim. Biophys. Acta.* 1436:19–33.

Timerman, A.P., H. Onoue, H.B. Xin, S. Barg, J. Copello, G. Wiederrecht, and S. Fleischer. 1996. Selective binding of FKBP12.6 by the cardiac ryanodine receptor. *J. Biol. Chem.* 271:20385–20391.

Wang, Y.X., Y.M. Zheng, I. Abdullaev, and M.I. Kotlikoff. 2003. Metabolic inhibition with cyanide induces calcium release in pulmonary artery myocytes and *Xenopus* oocytes. *Am. J. Physiol. Cell Physiol.* 284:C378–C388.

Xin, H.B., K. Rogers, Y. Qi, T. Kanematsu, and S. Fleischer. 1999. Three amino acid residues determine selective binding of FK506-binding protein 12.6 to the cardiac ryanodine receptor. *J. Biol. Chem.* 274:15315–15319.

Xin, H.B., T. Senbonmatsu, D.S. Cheng, Y.X. Wang, J.A. Copello, G.J. Ji, M.L. Collier, K.Y. Deng, L.H. Jeyakumar, M.A. Magnuson, et al. 2002. Oestrogen protects FKBP12.6 null mice from cardiac hypertrophy. *Nature.* 416:334–338.

ZhuGe, R., S.M. Sims, R.A. Tuft, K.E. Fogarty, and J.V. Walsh Jr. 1998. Ca2+ sparks activate K+ and Cl-channels, resulting in spontaneous transient currents in guinea-pig tracheal myocytes. *J. Physiol.* 513:711–718.